J Mol Model (2016) 22: 28
DOI 10.1007/s00894-015-2898-4

ORIGINAL PAPER

Self-stability of C_{60} nanocapsules with radio-iodide content and its interaction with calcium atoms

Alejandro Valderrama[1,2] · **Radamés Reynoso**[1] · **Raúl W. Gómez**[2] · **Vivianne Marquina**[2]

Received: 21 September 2015 / Accepted: 21 December 2015 / Published online: 9 January 2016
© Springer-Verlag Berlin Heidelberg 2016

Abstract This paper inquires the C_{60} capabilities to contain radio-iodide ($^{131}I_2$) molecules. The encapsulation conditions are investigated applying first principles method to simulate with geometric optimizations and molecular dynamics at 310 K and atmospheric pressure. We find that the $n^{131}I_2@C_{60}$ system, where n = 1, 2, 3…, is stable if the content does not exceed three molecules of radio-iodide. The application of density functional theory allows us to determine that, the nanocapsules content limit is related with the amount of charge that is transferred from the iodine $^{131}I_2$ molecules to the carbon atoms in the fullerene surface. The Mulliken population analysis reveals that the excess of charge increases the repulsive forces between atoms and the bond length average in the C_{60} structure. The weakened bonds easily break and will critically damage the encapsulation properties. Additionally, we test the interaction nanocapsules with different amounts of radioactive iodine diatomic molecules content with calcium atoms, and find that only the fullerene containing one radioactive iodine diatomic molecule was able to interact with up to nine atoms of calcium without disrupting or cracking. Other fullerenes with two and three radio iodine diatomic molecules cannot resist the interaction with a single calcium atom without cracking or being broken.

✉ Alejandro Valderrama
alecvald@ciencias.unam.mx

[1] Centro de Investigación en Ciencia Aplicada y Tecnología Avanzada Unidad Legaria, Instituto Politécnico Nacional, Calzada Legaria No. 694, Colonia Irrigación, Delegación Miguel Hidalgo C. P. 11500, D. F., Mexico

[2] Facultad de Ciencias, Universidad Nacional Autónoma de México, Avenida Universidad No. 3000, Ciudad Universitaria, Delegación Coyoacán C. P. 04510, D. F., Mexico

Keywords Buckminsterfullerene · Calcium physisorption · C_{60} · Nanocapsule · Radio-iodide

Introduction

The use of nanoparticles and carbon nanostructures as multifunctional carriers for biomedical applications has been put forward by several research works [1, 2]. This allows the encapsulation of radioactive compounds with a potential application on the treatment of tumors to be used in new nanodesigned drug delivery platform. To use nanocapsules within the human body, it is primordial to establish the suitable nanotubes sizes, and their storage capacity limit [3–5]. Being that fullerene C_{60} is a particular case of a nanotube and largely retains their properties [6, 7], it is convenient to study the properties of these structures in order to extend the results to design a molecular system larger and more complex [8, 9]. The C_{60} fullerene may be used as nanocapsules with a radioactive content and, with a proper treatment, its journey through the human body could be such as to prefer some tissues over others [10]. For example, the radio-iodide (^{131}I) could be used in such a way as to avoid its natural affinity with the thyroid tissue [11].

Notwithstanding the fact that localized treatments do not distinguish between healthy and unhealthy cells, through statistical studies of these treatments a balance of the abnormal growth rate of affected tissue can be achieved by the exposure to radio-doses. In fact, at present the radioactive treatments for thyroid cancer are successful enough, to make this disease the least lethal cancer [12]. It is then desirable to be able to extend these treatments to other tissues of the human body.

Bearing this in mind and knowing that bone metastases are extremely frequent, for which it is estimated that 350,000 people die annually in the U.S. [13] at least. And where bone

tissue appears to be the target of metastasis in 95 % of multiple myeloma patients, 75 % of patients with breast and prostate cancers, and 30–40 % in patients with lung cancer, the main purpose of our study is to simulate a nanocapsule containing radioactive iodine-131 [14] (which has a widespread use for treatment of hyperthyroidism and thyroid cancer) that can be functionalized with calcium atoms that will redirect the nanocapsule to the bone tissue so that traveling through the bloodstream can be fixed to the bone and allow localized radioactive medication.

Bone tissue is composed in equal parts (by volume) of a stretchable fibrous protein, called collagen, and brittle mineral phase, called hydroxyapatite (HA) [15]. So the molecular recognizer in the nanocapsule may consist of calcium atoms physisorbed on its surface with chemical affinity to hydroxyapatite present in bone tissue, so that the nanocapsules can be fixed to the bone [16, 17].

In this article we present for radio-iodide molecular encapsulation (#^{131}I@C_{60}) very similar results to those presented above for encapsulation within sodium radio-iodide (#Na^{131}I@C_{60}) [18] and some other tests with potassium radio-iodide (#K^{131}I@C_{60}). Thus, it is possible to determine in each case, a limit of fullerene molecules contained.

The fullerene encapsulation limit is established when it contains a number of atoms or molecules inside that causes instability, it cracks or breaks so that it loses its fundamental properties of storage, and can release some of its content to the medium. The interesting thing here is that this limit is not volumetric and does not depend on the mechanical and elastic fullerene ability to deform and restore its form [19, 20].

In all studied cases the reason that an encapsulation limit occurs is the donation of the valence electronic charge of the compounds stored in the cage, as has been pointed out in other studies [21, 22]. So encapsulation limit is due to a failure of the structure of the fullerene generated when repulsive charge accumulates on its surface. Therefore this encapsulation limit not only depends on the number of molecules inside the fullerene, but it will also depend, as shown below, on the electrical charges that are donated to fullerene by atoms or molecules that interact therewith by outside.

Delivery of these molecules to specific areas within the body will reduce systemic side effects and allow for more efficient use in the radioactive treatment. Nevertheless it is necessary that the nanostructured drug carriers be robust enough to guarantee its own integrity to accomplish their mission. No nanocapsule disruption, with a concomitant release of its content, can be acceptable during its bloodstream journey [23]. For this reason it is important to determine its molecular transport and storage capabilities before the functionalization process [24].

Thinking to redirect the nanocapsules with radio-iodide content to the bone tissue to deliver a radio doses in an osteosarcoma, we additionally proved that when the stable nanocapsules with molecular contents interacts with some calcium atoms, it presents critical conditions to maintain its integrity and encapsulation properties.

With no doubt will it be necessary to take actions in the redesign of these kinds of multi-functionalized molecular carriers to make them really useful. Leveraging its storage capacity as their tissue affinity capability within the body and modifying or improving their characteristics of stability, and durability for an adverse interaction medium.

Computational procedure

Geometry optimizations (GO) [25] that consists in a chemical structural determination on the electronic ground state and molecular dynamics (MD) that use initial temperature and a rescaling velocity parameter for thermalization, constitutes an important part of our quantum chemical calculations that were performed applying density functional theory (DFT) [26, 27] using norm-conserving pseudopotentials (PP) [28] of the type Perdew-Burke-Ernzerhof (PBE) [29] and an exchange-correlation scalar relativistic functional with Martins-Troullier [30] method.

We use supercomputing with Quantum Espresso v.4.3 (QE) [31] pw.x (Plane Wave Self-Consistent Field) parallel processing code to carry out heavy calculations. Further postprocessing was done with Amsterdam Density Functional (ADF) simple processing software for making graphical representations and to obtain the Mulliken electronic population analysis of the molecules, as well as of individual orbitals, both in terms of the elementary basis functions and the symmetry adapted fragment orbitals procedure [32]. Also we used GaussView 5.0.9 to compute the vibrational frequencies from the stable systems and obtain their IR spectral characterizations [33].

For all QE calculations the following valence electronic configurations were taken: $2s^2 2p^2$ for carbon, $5s^2 5p^5$ for iodine and $3s^2 3p^6 4s^2$ for calcium. We define a threshold for all forces with energy convergence of 0.1 meV for ionic minimization in a fixed-super cell system; and all computations were performed with an estimated SCF accuracy $< 9.0 \times 10 \wedge \{-5\}$ eV.

For the electronic structure calculations in the Brillouin zone we implemented super cell with a grid of eight irreducible k-points with the approximation to the occupation function using the Methfessel and Paxton method [34, 35].

The molecular dynamics calculations were made considering a rescaling process with a time step of 1 femtosecond to reach 310 K (as in the human body) at one atmosphere of pressure that was controlled by adding degrees of freedom for the cell size and volume with an application of the Parrinello-Rahman Lagrangian [36].

For all systems studied we perform scalar relativistic spin polarized and non-spin polarized calculations, and we got identical results so we establish that they are non-magnetic.

Usually the length of the carbon single (sp^3–sp^3) and double (sp^2–sp^2) bonds are reported at 1.54 Å and 1.34 Å respectively [37]. For C_{60} fullerene, Hare of the Sessex University reports average lengths of 1.455 Å for the C−C single bond, and 1.391 Å for the C=C double bond. [38]. In our case, with the GO estimation for the initial configuration of the fullerene C_{60} at the basic state we obtained the correct distribution of single and double bonds with average lengths: <d(C−C)>= 1.45 Å and <d(C=C)>0.140 Å. This makes a difference of about ± 0.01 Å from the values mentioned.

Likewise, we obtained the $^{131}I_2$ molecule covalent bond distance: d(I−I)=2.68 Å, which differs with respect to the common reported [39] value in ± 0.02 Å. These results reinforce the effectiveness of the method and pseudopotentials used in the geometrical optimizations and molecular dynamics.

For the formation energy of studied molecular systems we used the generic formula: $E_f = E_T - E_P$; where E_T is the molecular system total energy and E_P is the sum of the free particle energies. So, the average formation energy per atom in the system is $<E_A> = E_f/n$; where n is the number of atoms in the molecular system.

In this manner, the total energy which corresponds to the minimum C_{60}'s molecular energy at ground state, was found as $E_T = -9278.6506$ eV ≅ − 9.279 keV. So that, we obtained the molecular formation energy $E_f = -427.59$ eV. Therefore the average binding energy per atom is $<E_A> \cong -7.13$ eV.

Results and discussion

Geometrical optimization of C_{60} doped with $^{131}I_2$ molecules

With the C_{60} fullerene's configuration, this time as a starting point, optimization was performed with one to four molecules of radio-iodide ($^{131}I_2$) contained. The results found in the geometric optimizations are presented in Table 1, which shows the total energy corresponding to the minimum energy of the systems that are stable in the ground state, the system's formation energy which is responsible for the molecular cohesion, the formation energy per atom and in last column, and the carbon (single and double) bond length average.

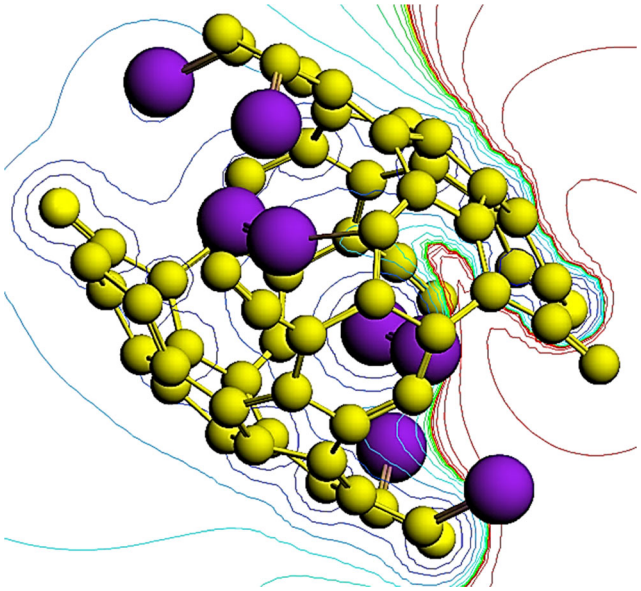

Fig. 1 Instability of $4^{131}I_2@C_{60}$. With four (or more) molecules of radioiodine the fullerene structure disrupts, and its content is released. The image also shows some potential curves also

As the radio-iodide content rises, the fullerene expands and the geometric structure of C_{60} is weakened. This increases the bond length between carbons and decreases the binding energy per atom. The average bond length became longer than the graphite bond type (≅1.42 Å), so that the stress in the structure increases as the structure weakens.

The case where the fullerene's content exceeded three radio-iodide diatomic molecules, i.e., ($4^{131}I_2$), proved to be unstable, the structure cannot resist the expansion breaking the fullerene and allowing the release of the initially contained molecules in the nanocapsule, as shown in Fig. 1.

C_{60}'s molecular dynamics with $^{131}I_2$ molecules contained

The molecular dynamics results at 310 K and atmospheric pressure for $^{131}I_2@C_{60}$, $2^{131}I_2@C_{60}$, and $3^{131}I_2@C_{60}$ are presented in Table 2.

The average binding energy per atom obtained in molecular dynamics at 310 K and atmospheric pressure for each system listed in the above table, differ by a small percentage (only about 0.6 %) of the average values obtained for ground

Table 1 C_{60} fullerene containing radio-iodide diatomic molecules geometrical optimization results

Optimization	E_T [keV]	E_f [eV]	$<E_A>$ [eV]	<d(C − C)>
$^{131}I_2@C_{60}$	−9.895	−421.03	−6.79	1.45 Å
$2^{131}I_2@C_{60}$	−10.489	−392.18	−6.13	1.50 Å
$3^{131}I_2@C_{60}$	−11.083	−362.52	−5.49	1.55 Å

Table 2 Total energy, molecular formation energy, and average binding energy per atom

Molecular dynamic	E_T [keV]	E_f [eV]	$<E_A>$ [eV]
$^{131}I_2@C_{60}$	−9.893	−418.66	−6.75
$2^{131}I_2@C_{60}$	−10.492	−394.82	−6.16
3^{131} $I_2@C_{60}$	−11.080	−359.56	−5.44

state. Therefore, these systems have not changed significantly in the considered temperature range (0 K, 310 K].

When we simulated heating of these endohedral systems with molecular dynamics to reach 310 K, the average binding energy per atom changes with each vibrational state. The increase of the vibrational amplitude causes the loss of cohesive energy. Qualitatively, however, the systems do not change so much and, the atomic bonds, in a single point of time, maintain approximately their length according the fullerene's stability at this level of temperature.

The next set of graphs in Fig. 2 shows the Calculating Cycles in the corresponding molecular dynamics.

Mulliken electronic charge distributions

We have obtained the empty C_{60} molecule Mulliken electronegativity [40], and also with one to three radio-iodide diatomic molecules inside.

Initially empty C_{60} is practically neutral. As the radio-iodide content rises, a minute shift transfer of negative charges from the iodine ^{131}I atoms toward the carbon atoms take place, see the series of images that follow the electronegativity's color scale in Fig. 3.

This produces some repulsion of the carbon atoms. In consequence, their binding energy diminishes, bonds become longer, and the structure is weakened.

In the case of nanocapsule $3^{131}I_2@C_{60}$ which has a higher amount of radioactive iodine, a simple analysis of the Mulliken's electronegativity values have revealed by an ADF-SP process, that there is a movement of negative charges in the iodine's molecules group $^{131}I_2$ inside

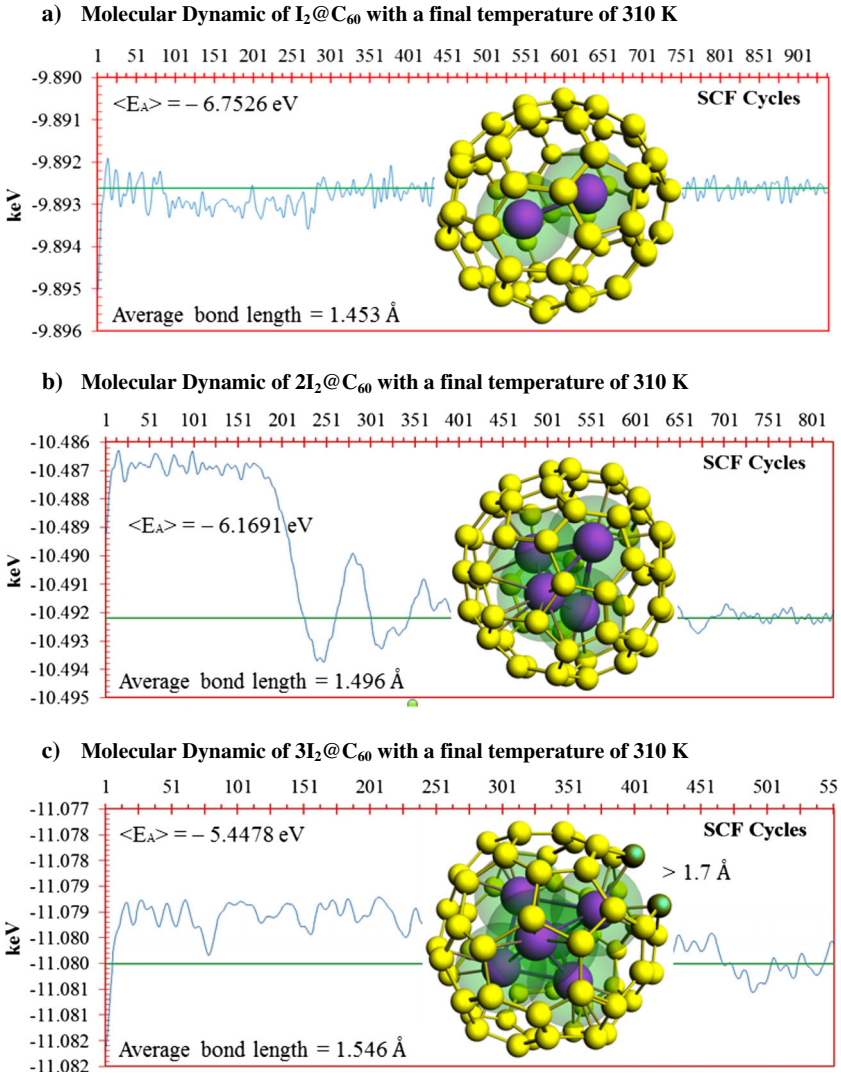

Fig. 2 Molecular dynamics of the systems $^{131}I_2@C_{60}$, $2^{131}I_2@C_{60}$, and $3^{131}I_2@C_{60}$ rescaling to reach 310 K as a final temperature. **a** When containing a diatomic molecule the fullerene undergoes a slight deformation in the radioiodine molecule axis direction. **b** With two radio diatomic iodine molecules inside, the fullerene undergoes, the binding energy of the fullerene decreases while it expands. **c** When it contains three molecules, the fullerene continues expanding and has five "anomalous links" > 1.7 Å. In the graphics, the green lines match the average

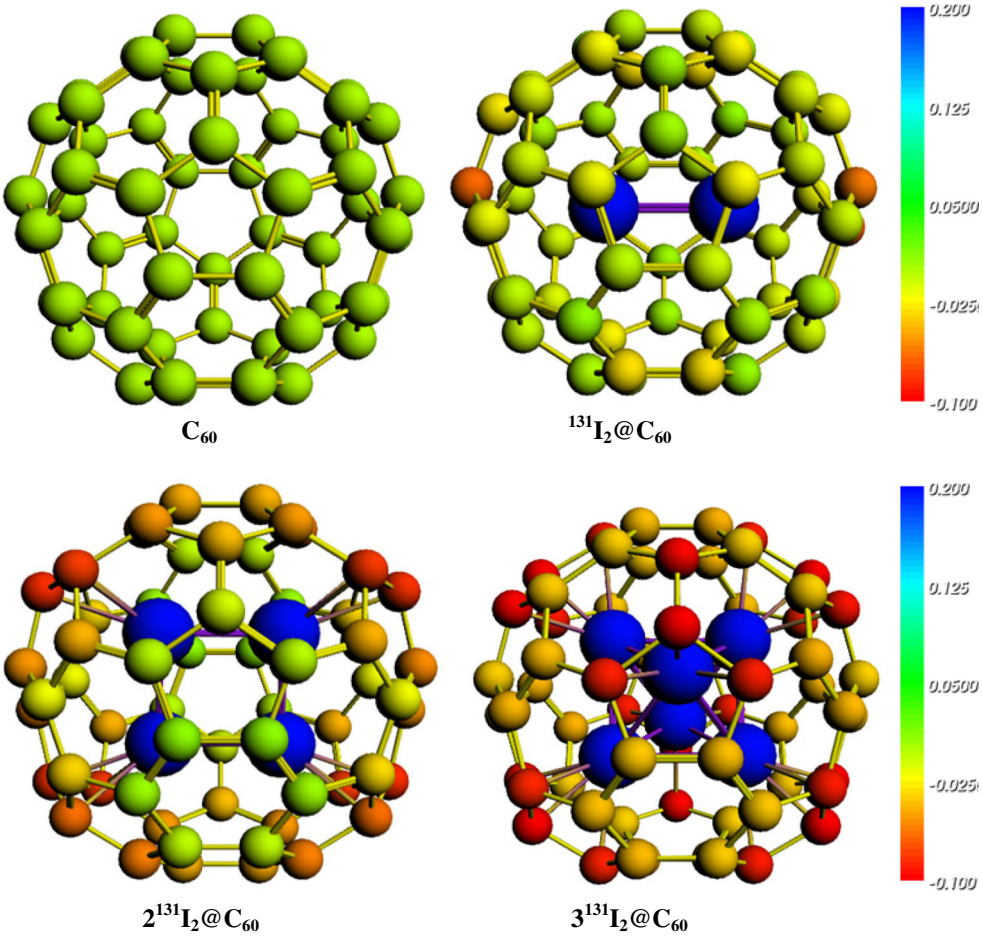

Fig. 3 Charge distribution trend on the Mulliken scale of the empty C_{60} and with one to three $^{131}I_2$ molecules inside

the fullerene, to buckyball's carbon atoms, as shown in Fig. 4.

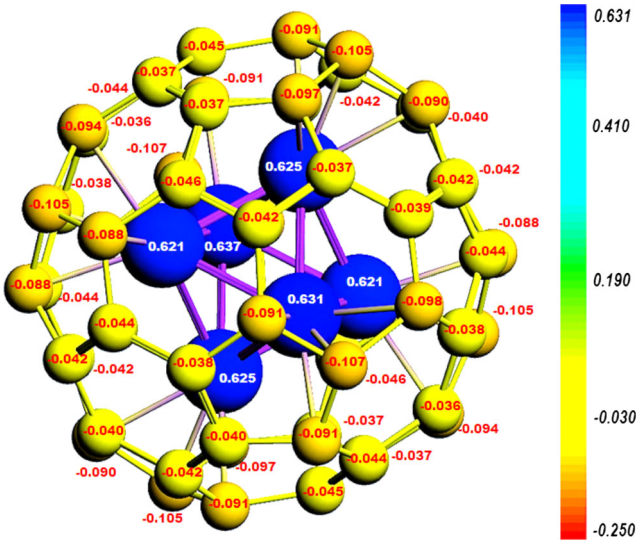

Fig. 4 Single point-ADF representation of the trend of positive charge distribution on Mulliken C_{60} scale system ($3^{131}I_2$). Inside the fullerene C_{60}, the iodine atoms tend to charge positively while some fullerene carbon atoms are negatively charged

C_{60}'s interaction with calcium atoms

Once the conditions for stable nanocapsules containing $^{131}I_2$ are delimit, we come up to the main purpose of this work: Can the fullerene adsorb calcium atoms without losing its stability?

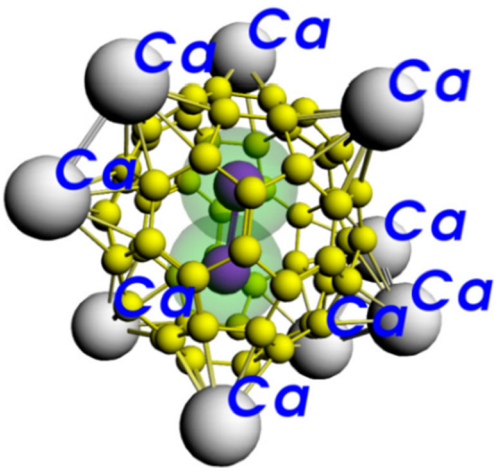

Fig. 5 Physisorption of nine calcium atoms by the nanocapsule with one radioiodine diatomic molecule, $^{131}I_2@C_{60}$

Table 3 Total energy, molecular formation energy, and average binding energy per atom by calcium's physisorption

Optimization	E_T [keV]	E_f [eV]	$<E_A>$ [eV]
$^{131}I_2@C_{60}$ Ca	−10.911	−422.88	−6.71
$^{131}I_2@C_{60}$ 2Ca	−11.928	−424.59	−6.63
$^{131}I_2@C_{60}$ 3Ca	−12.944	−425.90	−6.55
$^{131}I_2@C_{60}$ 4Ca	−13.959	−427.10	−6.47
$^{131}I_2@C_{60}$ 5Ca	−14.975	−428.41	−6.39
$^{131}I_2@C_{60}$ 6Ca	−15.992	−429.87	−6.32
$^{131}I_2@C_{60}$ 7Ca	−17.008	−431.62	−6.25
$^{131}I_2@C_{60}$ 8Ca	−18.025	−434.12	−6.20
$^{131}I_2@C_{60}$ 9Ca	−19.042	−435.711	−6.13

With the found stable nanocapsules we tested the interaction with some calcium atoms through a process of successive aggregation and we found that only the nanocapsules containing a single molecule of radioiodine, $^{131}I_2@C_{60}$, can physisorb some calcium atoms without losing their stability, as shown in Fig. 5.

The values of binding energy per atom of nanocapsule with one molecule of radioiodine contained for a different number of atoms of calcium physisorbed are presented in Table 3. As can be seen, the binding energy per atom values does not change much, so that the nanocapsule does not lose the stability.

The adsorption process of calcium by the nanocapsule surface with radioactive content, $^{131}I_2@C_{60}$, was performed successively. The adsorption energy of each calcium atom added did not change significantly, as shown in the following graph, see Fig. 6. Because calcium's atoms that adhere to the fullerene's surface and the fullerene retain their chemical nature, the adsorption process can be considered as a physisorption.

When a nanocapsule containing two radio diatomic iodine, $2^{131}I_2@C_{60}$, interacts with one to five atoms it shows cracks (the separation between the carbon atoms becomes greater than graphite bonds). For six or more calcium atoms, the average binding energy increases but the nanocapsule is broken.

The following graph, see Fig. 7, shows the average energy per atom of the interaction between $^{131}I_2@C_{60}$ and $2^{131}I_2@C_{60}$ systems with calcium atoms.

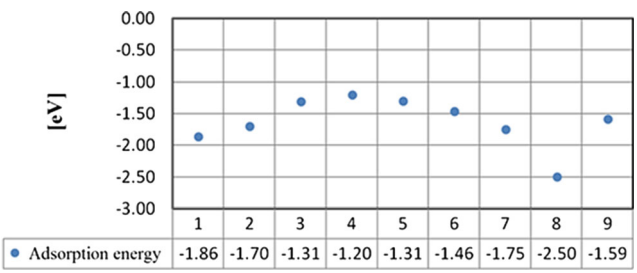

Fig. 6 The graphic shows that most calcium added to the $^{131}I_2@C_{60}$ nanocapsule has approximately the same adsorption energy

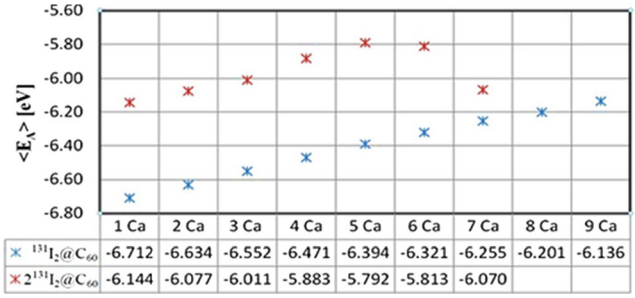

Fig. 7 Average binding energy per atom of calcium physisorption by the $^{131}I_2@C_{60}$ and $2^{131}I_2@C_{60}$ systems

Finally, the nanocapsule containing three radioactive iodine diatomic molecules, $3^{131}I_2@C_{60}$, easily disrupts when interacting with a single atom of calcium (see Fig. 8).

IR spectroscopy characterization

Since the C_{60} is a closed structure, the number of vibrational modes is given by $3\times60-6=174$, including translations and rotations. Due to the symmetry of C_{60}, there are 46 vibrational normal modes, 14 of them correspond to the ten active in Raman and four are in the IR range; the rest are optically null [41]. The value of the principal oscillation frequency has been reported with some variations within the range (526 cm^{-1}, 529 cm^{-1}) [42, 43].

As the content of the fullerene increases, its IR spectrum becomes more complex. At room temperature, the light carbon atoms oscillate at high frequencies, such that the fullerene has normal modes of vibration in the range (500 cm^{-1}, 1600 cm^{-1}), so only the fundamental states are significantly populated. However, vibrational energy differences between states of diatomic molecules of heavy atoms such as I_2 are small and stay basically in the interval (300 cm^{-1}, 800 cm^{-1}), so their excited states are significantly populated. This is shown in the graphs below.

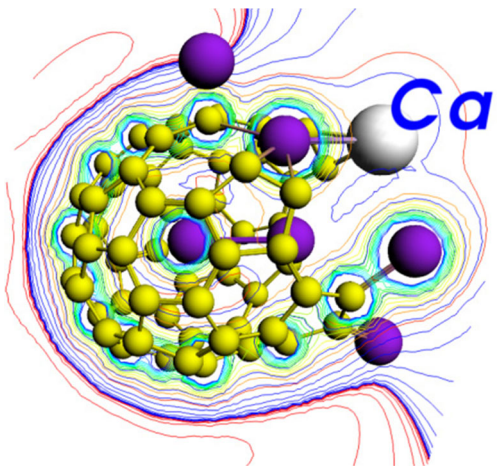

Fig. 8 Instability of $3^{131}I_2@C_{60}$ Ca. The image shows some potential curves also

IR Spectrums

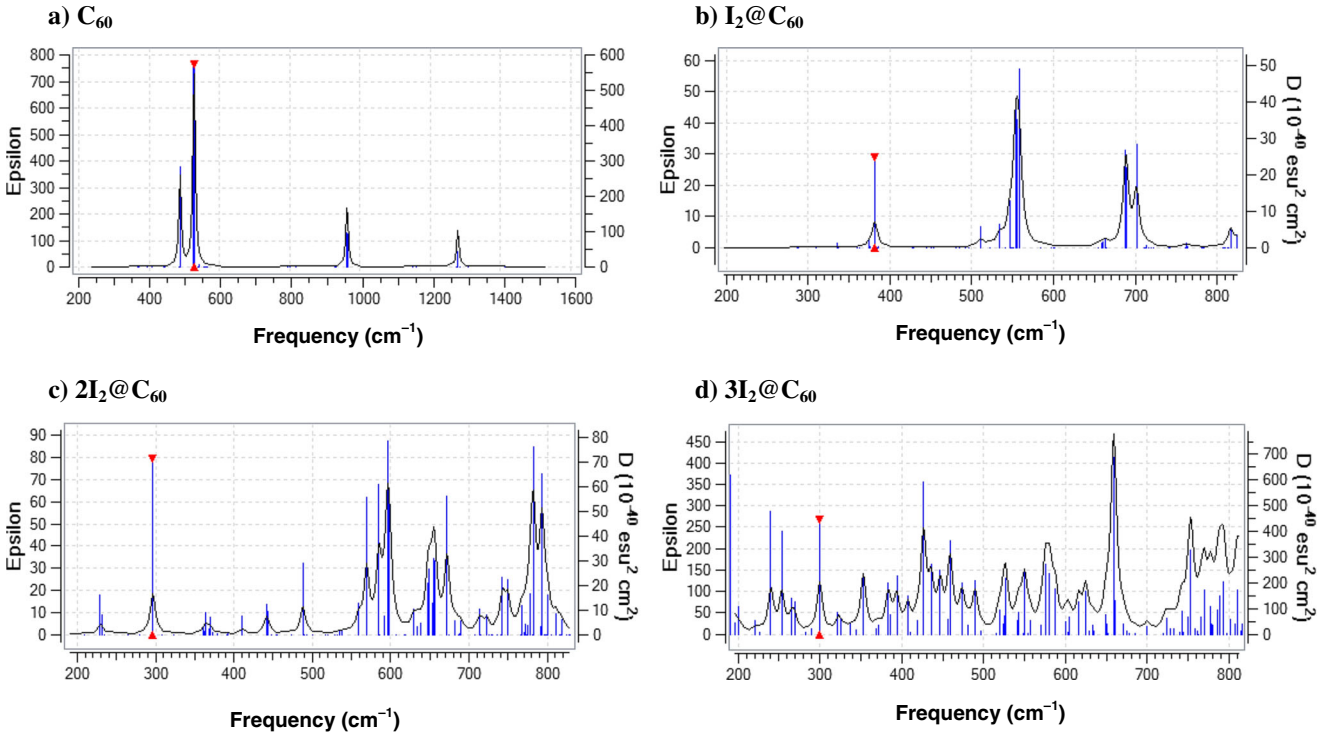

Fig. 9 The graphics present Gaussian's estimate of the IR spectrum for systems: **a**) C_{60}, **b**) $^{131}I_2@C_{60}$, **c**) $2^{131}I_2@C_{60}$, and **d**) $3^{131}I_2@C_{60}$. The intensity presented values are relative to the highest value in each molecular system and bear no precise relationship to experimental band intensities so its scaling is required to fit

With increasing diatomic iodine in the fullerene, the vibration modes begin to saturate in the region (300 cm^{-1}, 800 cm^{-1}) and the spectral energy increases significantly (see Fig. 9, sequence b to d).

In the IR spectrum of the system composed with the nanocapsule containing one molecule of radioactive iodine, and nine calcium atoms physisorbed, system [$^{131}I_2$ @ C_{60} + 9Ca], shown in Fig. 10, the overlapping regions may be associated in the following way: the first, of iodine diatomic molecules associated with low frequency; the second one, to the intermediate vibrational modes of the carbon atoms of fullerene; and, finally, the last one to the presence of calcium atoms with the region of vibrational modes greater than 1200 cm^{-1}, according to regions reported for calcium carbonate [44].

Again the system is very saturated so the spectral energy is very large and the system can be close to its limit of stability.

Conclusions

The DFT geometrical optimizations and molecular dynamics reported in this paper establish the feasibility of fullerene C_{60}

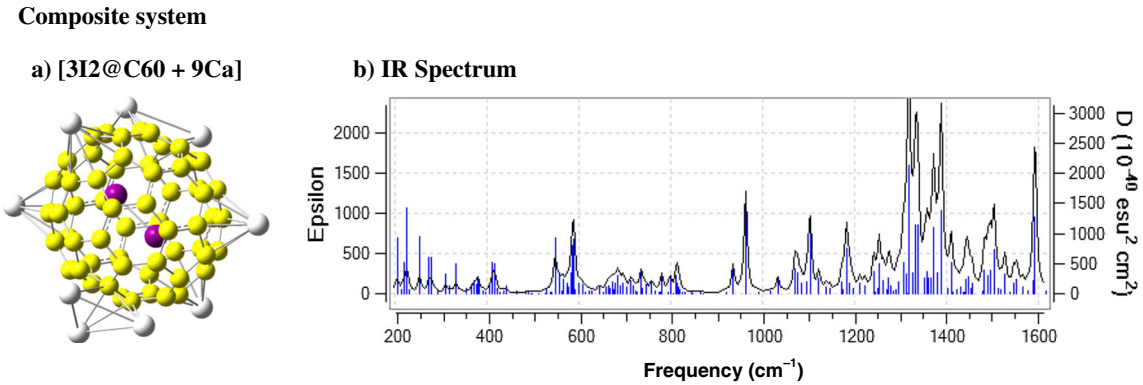

Fig. 10 **a** Nanocapsule $3I_2@C_{60}$ with 9Ca physisorbed. **b** IR spectrum of the composed system. **Notice:** The spectrums presented were calculated using a semi-empirical method based on the application of the Gaussian 09 standard integral processing infrastructure with PM6, PDDG, and PM3MM, and hence may differ in detail from calculus obtained with other methodology

to store up to three radio-iodide diatomic molecules, ($3^{131}I_2$), in an energetically stable form.

The Mulliken electronegativity analysis of the studied systems reveals that a small fraction of the electronic charge of the iodine atoms is transferred to the carbon atoms of the fullerene causing the expansion as the radio-iodide molecules content increases from one to three.

With respect to the stability of nanocapsules to interact with calcium, only the fullerene containing a single molecule of iodine was able to interact with atoms of calcium without disrupting. So only this kind of nanocapsule ($^{131}I_2@C_{60}$#Ca) could be used as a functional transporter.

It is important to note that, many studies have presented functionalized fullerenes, but is not usual to consider the conditions that can nullify their transporting properties. The study and design of nanocapsules must be predominant to ensure that they maintain their structural properties while they are in the blood stream.

So having a new platform that can supply nano doses in localized areas of the body requires a more complex molecular composition, of course based on drug encapsulation properties in fullerenes and nanotubes modified with a new, more robust structure and molecular recognition functions adapted as well as to include some atoms with optic, electric or magnetic characteristics to allow signaling and tracking functions.

Acknowledgements Special thanks to Consejo Nacional de Ciencia y Tecnología for the financial support given to this work in the national postdoctoral program and to NES-Miztli Supercomputer Center of the Dirección General de Tecnologías de la Información y Comunicación, Universidad Nacional Autónoma de México for their technical support on many of the computations performed.

References

1. Bohunicky B, Mousa SA (2010) Biosensors: the new wave in cancer diagnosis. Nanotechnol Sci Appl 2011(4):1–10. doi:10.2147/NSA.S13465
2. Mendes RG, Alicja B, Bernd B, Gianaurelio C, Rümmeli MH (2012) Carbon nanostructures as multi-functional drug delivery platforms. J Mater Chem B 2013(1):401–428. doi:10.1039/C2TB00085G. http://pubs.rsc.org/en/content/articlelanding/2013/tb/c2tb00085g#!divAbstract
3. Cleeland CS, Allen JD, Roberts SA et al (2012) Reducing the toxicity of cancer therapy: recognizing needs, taking action. Nat Rev Clin Oncol 9:471–478. doi:10.1038/nrclinonc.2012.99, http://www.ncbi.nlm.nih.gov/pubmed/22751283
4. Kostarelos K (2008) The long and short of carbon nanotube toxicity. Nat Biotechnol 26(7):774–6. doi:10.1038/nbt0708-774, http://www.nature.com/nbt/journal/v26/n7/full/nbt0708-774.html
5. Poland CA, Duffin R, Kinloch I et al (2008) Carbon nanotubes introduced into the abdominal cavity of mice show asbestos-like pathogenicity in a pilot study. Nat Nanotechnol 3:423–428. doi:10.1038/nnano.2008.111, http://www.nature.com/nnano/journal/v3/n7/abs/nnano.2008.111.html
6. Kroto HW, Heath JR, O'brien SC, Curl RF, Smalley RE (1985) C60: Buckminsterfullerene. Nature 318:162–163. doi:10.1038/318162a0, http://www.nature.com/nature/journal/v318/n6042/abs/318162a0.html
7. Dresselhaus MS et al. (1996). Science of fullerene and carbon nanotubes. Academic, New York. http://www.sciencedirect.com/science/book/9780122218200
8. Pan Zeng, Xue-Gui Yang, Jing Du (2006). Natural modes of C60 cage via carbon-carbon bonding element. Fract Nano and Eng Mater Struct pp 667–668. doi:10.1007/1-4020-4972-2_330
9. Johnson JF, Karthick M, Sathiesh Kumar S, Gopu G (2013). Carbon nanotubes as a cradle of impulse for implantable medical devices. The 15th International Conference on Biomedical Engineering vol 43 of the series IFMBE Proceedings pp 456–459. doi:10.1007/978-3-319-02913-9_116
10. Hong SY, Tobias G (2010) Filled glycosylated carbon nanotubes for in vivo radioemitter localization and imaging. Nat Mater 9:485–490. doi:10.1038/nmat2766, http://www.nature.com/nmat/journal/v9/n6/abs/nmat2766.html
11. Pauwels EK, Smit JW, Slats A, Bourguignon M, Overbeek F (2000) Health effects of therapeutic use of ^{131}I in hyperthyroidism. Q J Nucl Med 44(4):333–9. http://www.ncbi.nlm.nih.gov/pubmed/11302261
12. Braunstein GD (2012) Thyroid Cancer. doi:10.1007/978-1-4614-0875-8
13. Vicent S, Luis-Ravelo D, Antón I, Hernández I, Martínez S, de las Rivas J, Gúrpide A, Lecanda F (2006). Las metástasis óseas del cáncer. Anales del Sistema Sanitario de Navarra. 29:(2) http://scielo.isciii.es/scielo.php?script=sci_arttext&pid=S1137-66272006000300002
14. Health Physics Society North Carolina Chapter. NCHPS President Wendy Woehr. http://shop.perkinelmer.com/content/pdfs/english/iodine131.pdf
15. Grandfield K, McNally EA, Palmquist A, Botton GA, Thomsen P, Engqvist H (2010) Visualizing biointerfaces in three dimensions: electron tomography of the Bone-hydroxyapatite interface. J R Soc Interface. http://rsif.royalsocietypublishing.org/content/early/2010/06/08/rsif.2010.0213.full.pdf
16. Mann S (1988) Molecular recognition in biomineralization. Nature 332:119–124. doi:10.1038/332119a0, http://link.springer.com/chapter/10.1007%2F978-4-431-68132-8_8
17. Samachson J (1967) Mechanism for the exchange of the calcium in bone mineral. Nature 216:193–194. doi:10.1038/216193a0, http://www.nature.com.pbidi.unam.mx:8080/nature/journal/v216/n5111/pdf/216193a0.pdf
18. Valderrama A, Guzman J (2014) Encapsulation of sodium radio-iodide in fullerene C60. J Mol Model. doi:10.1007/s00894-014-2130-y, http://link.springer.com/article/10.1007%2Fs00894-014-2130-y#
19. Brenner DW, Harrison JA, White CT, Colton RJ (1991) Molecular dynamics simulations of the nanometer-scale mechanical properties of compressed Buckminsterfullerene. Thin Solid Films doi:10.1016/0040-6090(91)90425-W, http://www.sciencedirect.com/science/article/pii/004060909190425W
20. Shen H (2006) The compressive mechanical properties of C60 and endohedral M@C60 (M = Si, Ge) fullerene molecules. Elsevier Mater Lett. doi:10.1016/j.matlet.2005.12.077, http://www.researchgate.net/publication/257008289_The_compressive_mechanical_properties_of_C60_and_endohedral_MC60_(MSi_Ge)_fullerene_molecules
21. Lu J, Zhang X, Zhao X (2000) Relativistic electronic structure calculations on endohedral Gd@C60, La@C60, Gd@C74, and La@C74. Applied Physics A 70(4):461–464. http://link.springer.com/article/10.1007%2Fs003390051068

22. Zhong X et al (2010) Can single-atom change affect electron transport properties of molecular nanostructures such as C60 fullerene? J Phys Chem Lett 2010(1):1584–1589. doi:10.1021/jz100360t, http://phy.mtu.edu/pandey/publications/ZPRK2010_0.pdf
23. Hughes GA (2005) Nanostructure-mediated drug delivery. Nanomedicine: Nanotechnol Biol Med 1(1):22–30. doi:10.1016/j.nano.2004.11.009
24. Claes-Henrik A (2011). Chemistry of carbon nanostructures: functionalization of carbon nanotubes and synthesis of organometallic fullerene derivatives. Uppsala University http://www.diva-portal.org/smash/get/diva2:444118/FULLTEXT01.pdf
25. Schlegel HB (2011) Geometry optimization. Wiley, New York. doi:10.1002/wcms.34
26. Hohenberg P, Kohn W (1964) Inhomogeneous electron gas. Phys Rev 136:B864–B871. doi:10.1103/PhysRev.136.B864
27. Parr RG, Yang W (1989) Density-functional theory of atoms and molecules. Oxford Univ Press 76–77. https://global.oup.com/academic/product/density-functional-theory-of-atoms-and-molecules-9780195092769?cc=mx&lang=en&
28. Giannozzi P (2007) Notes on pseudopotential generation. Scuola Normale Superiore di Pisa. http://www.quantum-espresso.org/wp-content/uploads/Doc/pseudo-gen.pdf
29. Perdew JP, Zunger A (1981) Self-interaction correction to density-functional approximations for many-electron systems. Phys Rev B 23:5048–79. doi:10.1103/PhysRevB.23.5048
30. Troullier N, Martíns JL (1991) Efficient pseudo potentials for plane-wave calculations. Phys Rev B 43:1993–2006. http://www.tddft.org/TDDFT2004/PracticalSessions/papers/troullier_prb43.1993.pdf
31. Giannozzi P, Baroni S, Bonini N, Calandra M, Car R, Cavazzoni C et al (2009) Quantum espresso: a modular and open-source software project for quantum simulations of materials. J Phys Condens Matter 21:395502–19. http://research.cems.umn.edu/wentzcovitch/papers/J._Phys._Condens._Matter_21_395502_(2009).pdf
32. ADF Program System (2014) Scientific computing & modelling. NV Vrije Universiteit, Amsterdam, The Netherlands. http://www.scm.com/Doc/Doc2014/ADF/ADFUsersGuide/page319.html
33. Methfessel M, Paxton A (1989) High-precision sampling for Brillouin-zone integration in metals. Phys Rev B 40:3616. doi:10.1103/PhysRevB.40.3616
34. Roy Dennington, Todd Keith, and John Millam (2009) GaussView V 5.0.9. Semichem Inc, Shawnee Mission, KS. http://www.gaussian.com/g_tech/gv5ref/gv5citation.htm
35. Björkman T, Granäs O (2011) Adaptive smearing for brillouin zone integration. Int J Quantum Chem 111(5):1025. doi:10.1002/qua.22476, http://www.researchgate.net/publication/225070997_Adaptive_Smearing_for_Brillouin_Zone_Integration
36. Parrinello M, Rahman A (1981) Polymorphic transitions in single crystals. A new molecular dynamics method. J Appl Phys 52:7182. http://adsabs.harvard.edu/abs/1981JAP...52.7182P
37. Carey FA, Sundberg RJ (2007) Advanced organic chemistry part A: structure and mechanisms 5th edn. Springer, Heidelberg http://ocw.mit.edu/courses/chemistry/5-12-organic-chemistry-i-spring-2003/lecture-handouts/04.pdf
38. Hare J et al. (2015) Some properties of carbon and C60. http://www.creative-science.org.uk/propc60.html
39. Wells AF (1984) Structural inorganic chemistry. Clarendon, Oxford.
40. Putz MV, Russo N, Sicilia E (2005) About the Mulliken electronegativity in DFT. Theor Chem Accounts 114(1):38–45. doi:10.1007/s00214-005-0641-4, http://link.springer.com/article/10.1007%2Fs00214-005-0641-4#
41. Tlahuice Flores, Alfredo y Pérez Tijerina, Eduardo y Mejía Rosales, Sergio (2007). Modos vibracionales de C_{60} obtenidos mediante el método DFT. Ciencia UANL, 10 (3). http://eprints.uanl.mx/1815/
42. Kratschmer W, Lamb LD, Fostiropoulos K, Huffman DR (1990) Solid C60: a new form of carbon. Nature 347:354–357. http://www.nature.com/nature/journal/v347/n6291/abs/347354a0.html
43. Schettino V, Pagliaci M, Ciabini L, Cardini G (2001) The vibrational spectrum of fullerene C60. J Phys Chem A 105:11192–11196. doi:10.1021/jp012874t
44. Coblentz Society Collection (2009) http://webbook.nist.gov/cgi/cbook.cgi?ID=B6004659&Mask=80#IR-Spec